Rare Metal Materials and Engineering
Volume 48, Issue 10, October 2019
Available online at www.rmme.ac.cn

Science Press

Cite this article as: Rare Metal Materials and Engineering, 2019, 48(10): 3167-3174.

ARTICLE

Influence of Elemental Sulfur on the Corrosion Behavior of Alloy G3 in H_2S+CO_2 Saturated Chloride Solution

Fan Zhou[1], Wang Ziyu[1], Liu Jianyi[2], Huang Taiyu [1], Zhao Xing[1], Hu Xiaogang[3]

[1] Southwest Petroleum University, Chengdu 610500, China; [2] State Key Laboratory of Gas Reservoir Geology and Exploitation, Chengdu 610500, China; [3] Chongqing HKC Optoelectronics Technology Co. Ltd, Chongqing 401346, China

Abstract: Electrochemical microscope (SECM), scanning electron microscopy (SEM) and electrochemical impedance spectroscopy (EIS) were used to study the nickel-based alloy G3's corrosive behavior in various sulfur states in a medium environment containing H_2S, CO_2, Cl^- at room temperature (25 °C) and high temperature (90 °C). The results show that the corrosion degree becomes more serious with the increasing temperature, and slight pitting appears on the surface of the nickel-based alloy G3; the anode polarization curve has a passivation region at room temperature, and the active dissolution appears and passivation phenomenon disappears at a temperature of 90 °C. The X-ray diffraction indicates that the passivation film formed on the nickel-based alloy G3 is mainly composed of oxides of Ni, Cr and Fe. The passivation film is dissolved due to the S^{2-} intrusion film, the corrosion products are composed of NiS and FeS_2, and the G3 alloy's corrosion resistance is weakened in the sulfur-containing environment. Compared with the deposition and precipitation of sulfur, the suspended sulfur has the densest passivation film and the least corrosion. Studies have shown that sulfur is a strong oxidant, and its existence leads to severe local corrosion. The state of elemental sulfur is a key factor affecting the compactness and growth rate of corrosion product membranes, and also a key factor affecting the corrosion rate of alloys.

Key words: nickel-base alloy G3; corrosion behavior; polarization curve; impedance spectrum; passive films; corrosion morphology

Currently the high-sulfur gas field containing H_2S and CO_2 is an important source of natural gas in global oil and gas exploration, and also an enriched area of sulfur[1]. CO_2 and H_2S in the well is extremely corrosive, and H_2S is highly toxic[2], so there are a series of problems in the corrosion resistance of metal in highly corrosive environments. For example, Chuanyu oil and gas field has the problems of high-temperature, high formation pressure, high-partial pressures of CO_2 and H_2S, and high content of Cl^-, which may lead to sulfide stress-cracking, sulfide corrosion-cracking and hydrogen induced-cracking which destroy the tubing and pipe rapidly[3]. Thus, materials of tubing and pipe are especially crucial for acid gas wells which contain high partial pressure of H_2S/CO_2 and elemental sulfur. Considering the safety, only high alloy stainless steel or nickel-base alloy tubing and casing products can be used under severe conditions[4-6]. The nickel-base corrosion resistant alloy is a category of corrosion resistant material with high-performance due to its superior localized corrosion resistance, the main elements of which include Ni, Cr, and Mo[3,7]. Chromium is used to promote the formation of a stable passive oxide layer which is highly resistant to corrosion[8]. Molybdenum is also added to promote resistance to pitting and inter granular corrosion[9-11]. Nickel-base alloys have been used in corrosive acidic gas field, and many published papers have focused on the nickel-base alloys in high temperature, high pressure water both in dynamic flowing conditions or in static autoclaves[12-16]. But there are not many reports about the corrosion behavior of nickel-base alloys in co-existence environment of H_2S, CO_2, Cl^- and S. The purpose of this paper is to investigate the

Received date: October 17, 2018
Foundation item: National Natural Science Foundation of China (51474181); State Key Laboratory of Oil/Gas Reservoir Geology and Exploitation Open Fund Project (PLN1516)
Corresponding author: Fan Zhou, Master, Associate Professor, School of Materials Science and Engineering, Southwest Petroleum University, Chengdu 610500, P. R. China, Tel: 0086-28-83037416, E-mail: fanzhou505@163.com

corrosion behavior of the nickel-base alloy G3 at different temperatures in simulated corrosion environment containing H_2S,CO_2, S and Cl^-, and the influence of elemental sulfur on the behavior of corrosion, further to reveal the corrosion mechanisms of alloy G3 in high-sulfur gas field.

1 Experiment

The chemical composition of nickel-base alloy G3 used for substrate material in this study is as follows (wt%): Ni 41.94, Cr 21.75, Mo 3.25, Al 0.18, Co 0.32, Mn 0.51, Si 0.10, Ti 2.07, Cu 1.72, C 0.02, Fe bal. G3 alloy has a single-phase austenite microstructure (as shown in Fig.1) with high corrosion resistance, which has been used in oil and gas wells in H_2S-Cl^- environments[17-19].

The immersion test and electrochemical measurements were used to assess the corrosion behavior of the experimental alloys. The samples for immersion test were 30 mm×15 mm×3 mm, and the samples for electrochemical measurements were 10 mm×10 mm×3 mm. All of the samples were abraded, polished and degreased.

The specimens for immersion test were immersed in H_2S+ CO_2 saturated chloride solution at room temperature (25 °C) and high temperature (90°C) for 168 h. After deoxygenated by pure nitrogen for 2 h, 3.5% NaCl solution was saturated by H_2S and CO_2. The saturate partial pressure of H_2S was 9 MPa and the saturate partial pressure of CO_2 was 6 MPa in accordance with the alloy G3 in-service environment. For investigating the influence of sulfur in different states on the corrosion behavior of the experimental alloys, a certain amount of elemental sulfur was deposited (as deposited sulfur) or precipitated (as precipitated sulfur) on the surface of the samples, and suspended with concentration of 10 g/L in the experimental solution by stirring (as suspended sulfur). The deposited sulfur is the elemental sulfur melted at 135 °C by heating and coating on the surface of the sample, while the preci- pitated sulfur is the elemental sulfur dissolved in toluene to saturation and precipitated on the surface of the sample until toluene volatilization. The conditions of immersion test and electrochemical measurements for G3 are shown as Table 1.

The surface morphology and microstructure of specimens

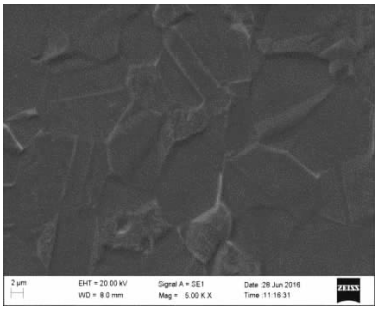

Fig.1 SEM image of nickel-base alloy G3

Table 1 Conditions of immersion test and electrochemical measurements for nickel-base alloy G3 in 3.5%NaCl+ saturated H_2S/CO_2

Test No.	Temperature/°C	Elemental sulfur states
1	25	Sulfur-free
2	25	Suspended sulfur (10 g/L)
3	25	Deposited sulfur
4	25	Precipitated sulfur
5	90	Sulfur-free
6	90	Suspended sulfur (10 g/L)
7	90	Deposited sulfur
8	90	Precipitated sulfur

after immersion were observed and analyzed by SEM, XRD with ZEISS EV0 MA15 instrument and X Pert PRO MPD instrument. The electrochemical corrosion characteristics of G3 were investigated using a CHI604D electrochemical workstation and three electrode cell. Nickel-base alloy G3 was used as working electrode, platinum electrode as the counter electrode, and saturated calomel electrode (SCE) as the reference electrode. Potential dynamic polarization curves were obtained at a scan speed of 1 $mV{\cdot}s^{-1}$ and a scan range of –500 mV to +800 mV with the sample area of 1 cm^2. EIS analysis was performed under potential static conditions in a frequency range from 100 kHz to 0.01 Hz with amplitude of 10 mV AC signal. Also, the electrochemical measurements were carried out when the electrochemical system was in steady state.

SECM, a technique in which the current flows through a very small electrode tip near a conductive, semi- conductive, or insulating substrate immersed in solution is used to characterize processes and structural features at the substrate as the tip is moved near the surface[20,21]. A CHI900C scanning electrochemical microscope with a 10 μm platinum tip as the probe, an Ag/AgCl/KCl (saturated) reference electrode, and a platinum counter electrode was employed to test the local corrosion area. The 6 mm cylinder specimens of G3 were used as study electrode. The polarization potential of the probe is 0.5 V, the distance between tip-substrate is 30 μm, and the scan range is 400 μm×400 μm.

2 Results and Discussion

2.1 Electrochemical measurements

Polarization curves in test 1 and 5 are shown in Fig.2a. It is clear that G3 has a passivation region at different temperatures. The E_{corr} values at 90 °C is more negative than that at room temperature (RT). The result indicates that with the increase of temperature, the surface activity at 90 °C is higher than that at RT, so the corrosion resistance is reduced. Beyond the E_{corr}, the anodic current increases rapidly until the passivation potential (E_p) is achieved, indicating that dissolution reaction contributes most to the current. After passing E_p, the anodic current remains unchanged and tends to hold until the potential reaches the

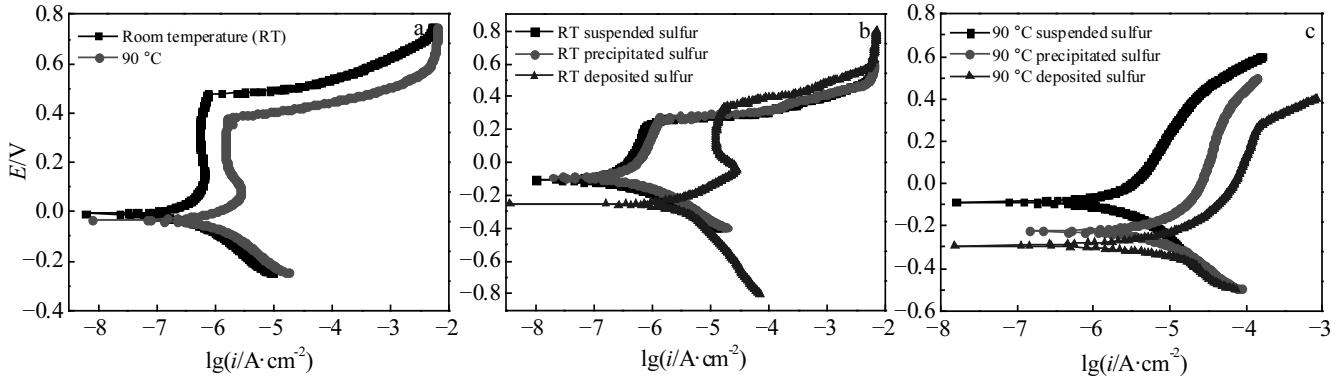

Fig.2 Potential dynamic polarization curves of alloy G3: (a) at different temperature without sulfur; (b) in various states of sulfur at room temperature; (c) in various states of sulfur at 90 °C

pitting one (E_{pit}). It is obvious from Fig.2a that the passivation region at RT is wider than that at 90 °C, and it is clear that the G3 at RT has stable passivation regions, the E_{pit} at RT is also higher and the passive current density at RT is also much smaller. The result indicates that a compact passive film forms, which covers alloy surface, and the active ion cannot contact with alloy.

Fig.2b shows the potential dynamic polarization curves of G3 in test 2~4. With the addition of sulfur, it can be seen that a little difference appears in polarization curves. It is clear that the specimen also has a passivation region, but the passive film is unstable and the I_{corr} increases slowly. The E_{corr} value in deposited sulfur environment is more negative than that in other environment. The result indicates that the surface activity in deposited sulfur environment is higher than that in other environment due to the formation of different films on the alloy surface. Comparing the polarization curves in test 1, 5 and the passivation region obtained in test 2~4, the later polarization curves have an unstable passivation region, the corrosion current increases gradually with the increasing potential, which suggests that the poor corrosion resistance of films formed in test 2~4.

Fig.2c shows the potential dynamic polarization curves of G3 in test 6~8. It is clear that the active dissolution and passivation phenomenon disappear. The self-corrosion potential in deposited sulfur state is more negative than that in other environment, and the self-corrosion current is the minimal. It suggests that the smaller driving force is required to initiate corrosion in the suspended sulfur state. Compared with the results in Fig.2b, the characteristic parameters of both E_{corr} and I_{corr} shift in a more negative direction. The result indicates that the depolarization effect of cathodic reaction increases in the sulfur environment, which increases the corrosion rate [5]. Comparing Fig.2a with Fig.2b from passive current density (I_{pass}), we can see that the I_{pass} values in presence sulfur case are larger than the ones in the absence sulfur case, which indicates that sulfur accelerates the corrosion attack of the nickel-base alloys suggesting that sulfur working as a cathodic depolarizer can accelerate the corrosion process.

This result reveals that the pitting corrosion resistance of alloy in absence sulfur environment is superior to that of the alloy in presence sulfur environment, and the critical pitting point value decreases with increasing the temperature. The adherent barrier with a greater thickness forms on the alloy surface. However, the breakdown of the passive film is due to the corrosion of aggressive environment such as test in sulfur environment, the pitting corrosion will also occur, and the corrosion resistance decreases rapidly.

Fig.3a and Fig.4a provide the impedance diagrams recorded after the formation of corrosion films on nickel-base alloys G3 by immersion tests in acid solution. The plots show similar capacitive responses over the entire frequency interval. For the immersion temperature and state of sulfur, the semicircle diameter decreases. These variations in Nyquist plots can be related to modifications in the thickness and porosity of the films formed on the alloy [22,23]. According to Fig.3, the corrosive resistance of G3 in suspended sulfur environment is the best. It indicates that the enrichment of sulfur element on the surface of the substrate has great influence on the corrosion resistance. In comparison with the results in the Fig.3a, although the capacitive order has no change, the capacitance semicircle diameter decreases obviously. It indicates that with the increase of temperature, the move of active ions becomes violent, which result in the partial acidification formation occluded corrosion cell so as to increase the corrosion.

The Bode plot analysis in Fig.3b, 3c and Fig.4b, 4c reflects the same tendency as Nyquist results for different samples. For both samples, only one capacitive loop is observed at 10 Hz. In order to study the film property of the alloy immersed in sour medium, a fitting procedure was carried out using an equivalent circuit, shown in Fig.5. The model used for fitting consists of the solution resistance (R_s), the charge transfer resistance (R_{ct}) of the interfacial corrosion reaction and the

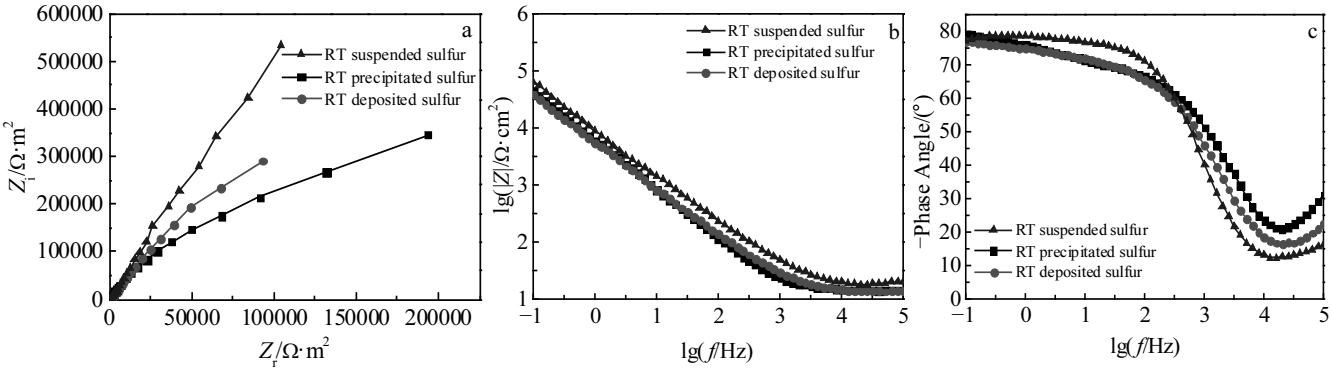

Fig.3 EIS plots of alloy G3 in various states of sulfur at RT: (a) Nyquist plots, (b) Bode lg|*Z*| vs lg*f* plots, and (c) Bode-phase angle vs lg*f* plots

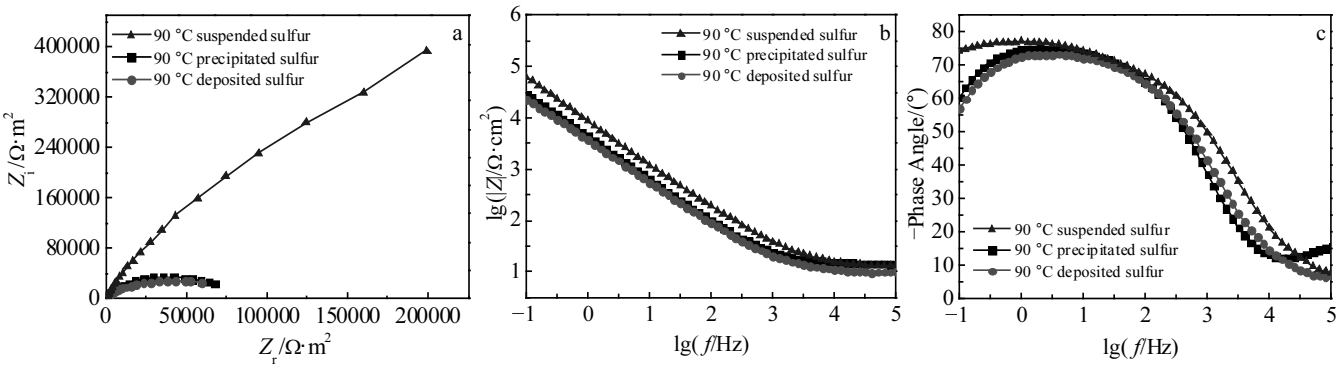

Fig.4 EIS plots of alloy G3 in various states of sulfur at 90 °C: (a) Nyquist plots, (b) Bode lg|*Z*| vs lg*f* plots, and (c) Bode-phase angle vs lg*f* plots

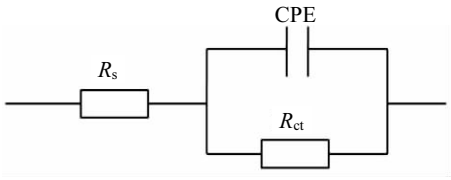

Fig.5 Equivalent circuit

constant phase element (CPE). The double layer capacitance on real cells often not a pure capacitor but like a CPE. A rough and porous alloy surface can cause double layer capacitance as CPE to appear [21]. The capacitance values were calculated using the equation [24]:

$$Z_{CPE}=Q^{-1}(j\omega)^{-n} \quad (1)$$

where Q is the magnitude of the CPE, j is the imaginary unit, ω is the angular frequency, and n is the phase shift which gives details about the degree of surface roughness[25].

The fitted parameter values are listed in Tables 2 and 3. The charge transfer resistance with the increase of temperature is significantly reduced about one to two orders of magnitude. Compared with suspended sulfur, the precipitated sulfur and

Table 2 Electrochemical parameters obtained from simulation of EIS plots of alloy G3 in various states of sulfur at RT

State	R_s/Ω·cm^2	CPE/ ×10^{-5} F·cm^2	n	R_{ct}/Ω·cm^2
Suspended sulfur	39.91	1.85	0.8347	7.3×10^{13}
Precipitated sulfur	28.02	2.974	0.8873	1.073×10^{6}
Deposited sulfur	31.54	3.53	0.8367	9.427×10^{11}

Table 3 Electrochemical parameters obtained from simulation of EIS plots of alloy G3 in various states of sulfur at 90 °C

Experiment	R_s/Ω·cm^2	CPE/ ×10^{-5} F·cm^2	n	R_{ct}/ ×10^4 Ω·cm^2
Suspended sulfur	13.87	3.394	0.8313	27.08
Precipitated sulfur	38.31	4.433	0.8586	8.486
Deposited sulfur	10.24	6.045	0.8103	8.076

deposited sulfur enrichment of sulfur on the surface of the substrate has great influence on the corrosion resistance, and Cl^- also plays a key role in accelerating and catalyze this process. Therefore, with the increase of temperature, the move of active ions becomes violent, which will result in the partial acidification formation occluded corrosion cell so as to decrease the impedance and increase the corrosion.

Fig.6 presents the morphologies of the specimens. From the RT test, the substrate surface current is smooth which indicates that there is no active pitting area and slight corrosion. However, as the sulfur states changes, the tip current increases. It indicates that with the changing of sulfur states, the substrate surface becomes active, which will result in the active dissolution so as to increase the corrosion. In 90 °C test, the surface of substrate began to exhibit obvious current fluctuation point, the micro-area current of deposited sulfur changes significantly increases by an order of magnitude. Compared with the current across RT and 90 °C, the corrosion condition becomes harsh, the active area and the pitting sensitivity also increases obviously. The conclusion is consistent with the above experimental results. Along with the increase of temperature, sulfur accelerates the corrosion attack of G3, suggesting that sulfur working as a cathodic depolarizer can accelerate the corrosion process. With the increase of the time, the pitting corrosion stable development, it has caused pitting corrosion pits gradually deepened and aggravated.

2.2 Structural and morphological studies

The morphologies of the specimen surface in Fig.7 show the product film in the various corrosion conditions. It indicates that the densities of the corrosion products under different sulfur states are different. At room temperature, the scales are relatively compact and smooth with flocculent particle stacking growth, the film in the suspended sulfur environment is also the most compact, and the alloy performs the best corrosion resistance in suspended sulfur state. But in 90 °C environment, the corrosion products are loose, porous and easy to fall off. Fig.8 shows the corrosion morphologies and the macrographs of surfaces of the two alloys after removal of the corrosion scales. The corrosion morphologies have great variation, and the corrosion resistance of alloys also turns worse.

At room temperature, the surface is less corroded and smooth with a homogeneous morphology. These results prove that the compact corrosion scale forms on the metal surface and can effectively protect G3 samples from a corrosive environment. However, an increase in the roughness and porosity of the films is observed as the temperature increases, the product films are loose and porous, and there are clear boundaries between the particles that provide a convenient channel for the layer internal and external material exchange. The suspended sulfur corrosion is slight. Precipitated and deposited sulfur corrosion pits appear to gather, woven into the complex network structure. The primary reason is that the product film is not dense, resulting in severe local corrosion. Moreover, under deposited sulfur condition, G3 even shows local corrosion cracks which indicates that the sulfur deposition forms have a great influence on the corrosion rate and the metal materials morphology. The sulfur direct contact with metal surface is the main reason that induces rapid corrosion and also

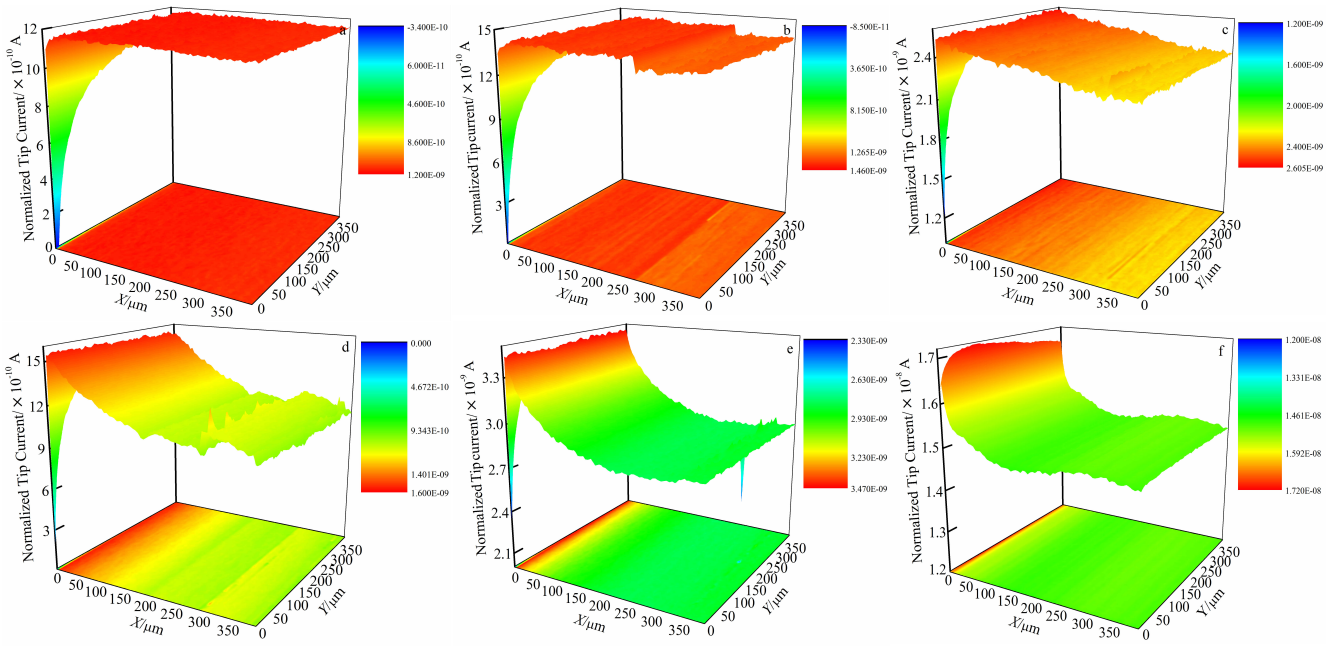

Fig.6 SECM 3D view: (a) RT suspended sulfur, (b) RT precipitated sulfur, (c) RT deposited sulfur, (d) 90 °C suspended sulfur, (e) 90 °C precipitated, and (f) 90 °C deposited sulfur

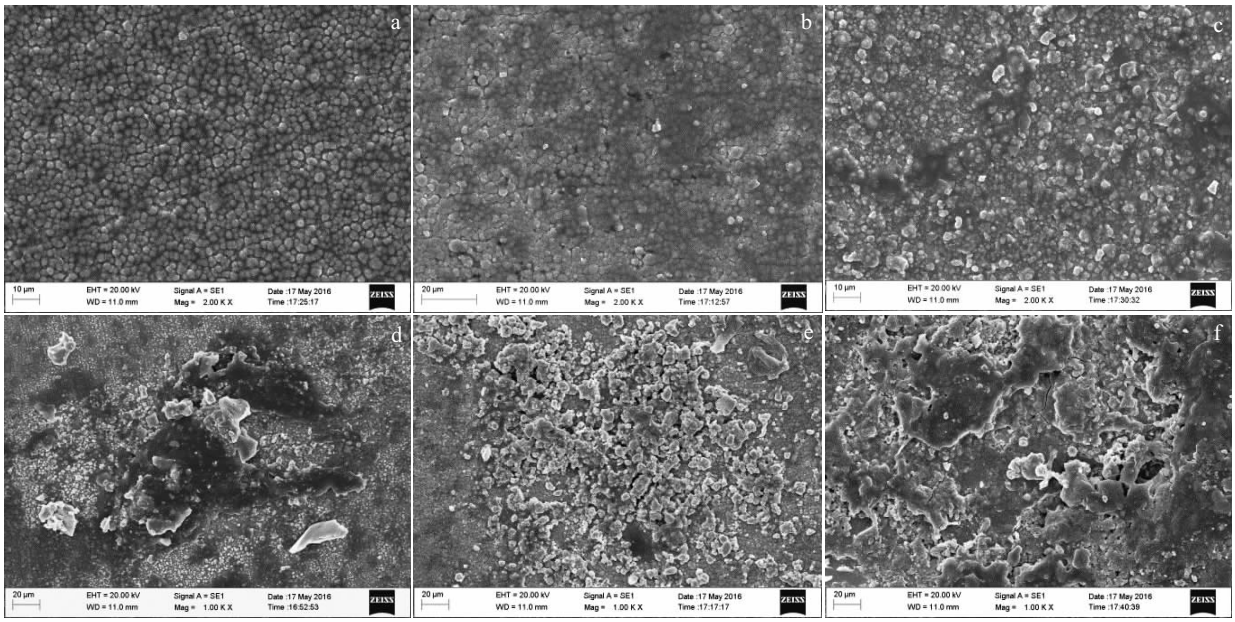

Fig.7 SEM images of corrosion films: (a) RT suspended sulfur, (b) RT precipitated sulfur, (c) RT deposited sulfur, (d) 90 °C suspended sulfur, (e) 90 °C precipitated sulfur, and (f) 90 °C deposited sulfur

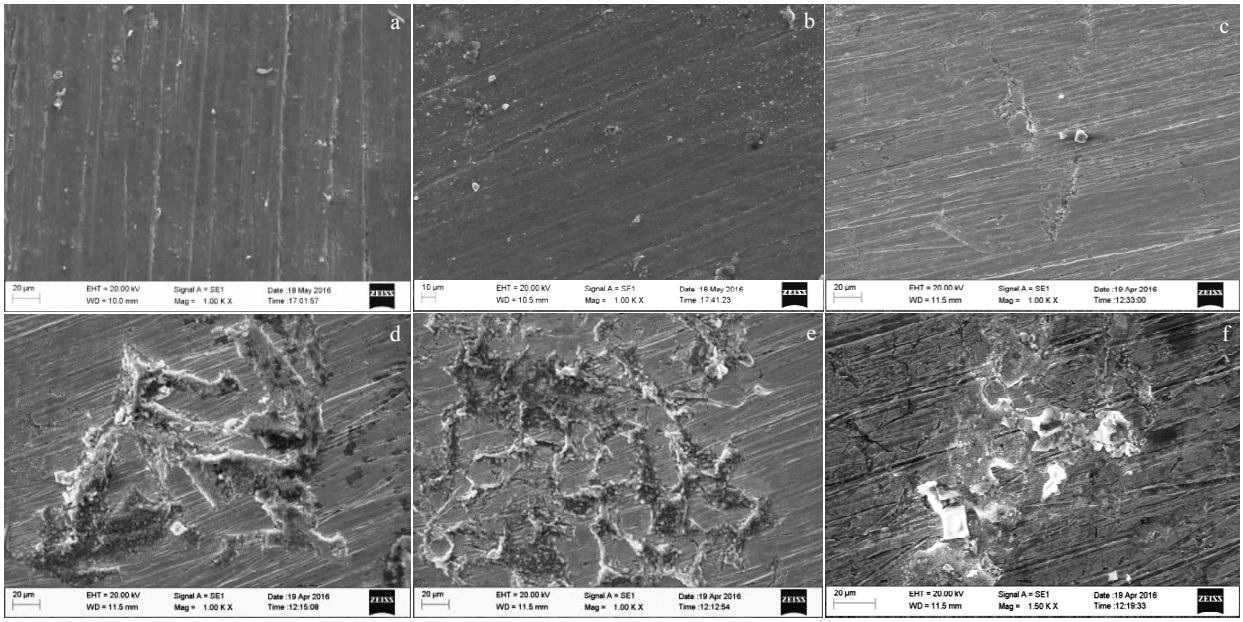

Fig.8 SEM images of substrate: (a) RT suspended sulfur, (b) RT precipitated sulfur, (c) RT deposited sulfur, (d) 90 °C suspended sulfur, (e) 90 °C precipitated sulfur, and (f) 90 °C deposited sulfur

is the indirect evidence that sulfur directly involved in corrosion electrochemical reactions, which has accelerated the corrosion process. The result indicates that the local corrosion caused by sulfur is closely related to the sulfur contact forms with materials.

Fig.9 shows the XRD patterns of the corrosion films on G3. We observe the presence of similar peaks at both temperatures. At room temperature, we note the presence of nickel sulfide (Ni_3S_2) and substrate alloy. However, when the temperature grows up to 90 °C, corrosion product begins to show a lot of different types, mainly including oxides and sulfides. It seems that the temperature slightly modifies the chemical composition

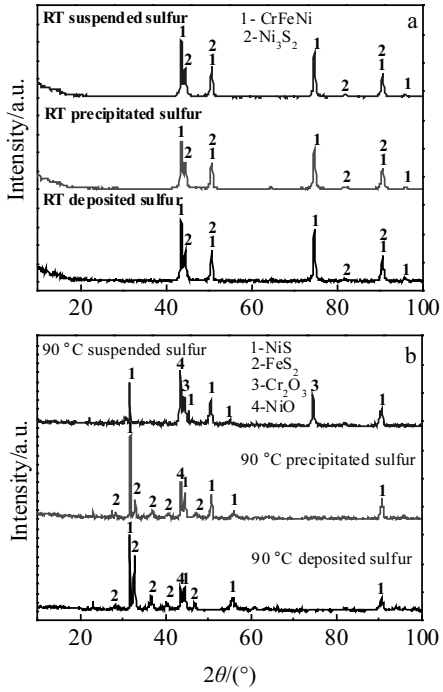

Fig.9 XRD patterns of the corrosion films in different conditions: (a) RT various states sulfur and (b) 90 °C various states sulfur

of the sulphide films. We note the presence of nickel sulfide (NiS), cubic pyrite (FeS_2), chromium oxide (Cr_2O_3) and nickel oxide (NiO).

The majority of strong peaks come from intermetallic compound of Fe/Ni/Cr, NiS substance, and some weak peaks of FeS_2, Cr_2O_3 and FeO occur in the patterns.

Nickel and chromium react with sulfur by outward diffusion of metal cations and inward migration of sulfur anions. The diffusivity of nickel is faster than that of chromium and thus the sulfidation rate of the former is higher than that of the latter. Therefore, as expected, there is a peak of NiS, and metal oxides are superior to precipitating on the surface[5]. Nickel oxide (NiO) is generally accepted as the main component in the passive film on nickel in both acidic and alkaline environments[26]. Okuyama and Haruyama[27] studied the passive film formed anodic alloy on nickel in borate buffer solution and concluded that NiO was responsible for passivity. In suspended sulfur environment, there are NiO and Cr_2O_3, while in precipitated sulfur and deposited sulfur environment NiO and Cr_2O_3 disappear. The change occurring in passive film is subjected to high temperature and a high level of sulfur is probably the chief mechanism for decline in the corrosion resistance capability of G3. Sulfur is a strong oxidant, and the presence of sulfur leads to a serious localized corrosion.

As mentioned above, in high temperature and high sulfur environment, the G3 passivation film has been eroded by the media and the corrosion resistance is reduced. At high temperature, sulfur in the case of a large content through the disproportion reaction can produce a large number of S^{2-} and HS^-. The equation is as follows:

$$4S+4H_2O\rightarrow 3H_2S+H_2SO_4\rightarrow 6H^++2HS^-+SO_4^{2-}+S^{2-} \quad (2)$$

According to Macdonald's point defect model [28], oxygen vacancies of passivation film migrate to the passivation film/solution interface, through Mott-Schottky pair reaction, resulting in the metal cations undergoing dissolution formed the metal sulphides FeS_2 and NiS. The polarity of S^{2-} is higher than that of Cl^-, the S^{2-} is likely to compete with Cl^- on the oxygen vacancies and gradually form a metal sulfide on the surface of the passive film, and the further reaction can cause the S^{2-} to migrate to the inner layer of the passive film. So the transition of the metal oxide passivation film to the sulfide passivation film may be the main reason for the corrosion resistance decreasing of nickel-base alloy G3. Also, S^{2-} can cause alkaline hydrolysis. With the increase of temperature, the hydrolysis is more serious formed hydroxide. While the hydroxide reacts with inner layer S^{2-} formed sulfides destroy stability of passive film. When the proton reaction of OH^- generates H^+ and O^{2-}, hydrogen ions move to the surface layer of the film. The O^{2-} enters into the inner layer of the film react with the metal ions to form oxide maintaining the stability of the passive film. We can infer that the passivation film is between the corrosive medium and the substrate, so as to reduce the corrosion medium ion attacking the substrate, the passive film stability is better at room temperature. However, at higher temperature, along with changing of the sulfur states the dissolution of the passive film occurs and the small anode large cathode forms, accelerating the corrosion. Origin of passive film of nickel-base alloy is as follows:

$$S^{2-}+Ni^{2+}\rightarrow NiS \quad (3)$$

$$HS^-+Ni^{2+}\rightarrow NiS+H^+ \quad (4)$$

$$S^{2-}+Ni(OH)_2\rightarrow NiS+2OH^- \quad (5)$$

$$NiO+2OH^-\rightarrow Ni(OH)_2+O^{2-} \quad (6)$$

$$Ni^{2-}+O^{2-}\rightarrow NiO \quad (7)$$

3 Conclusions

1) The G3 corrosion inhibition decrease with increasing the temperature, which may be attributed to the move of active ions becoming violent, which results in the partial acidification formation occluded cell so as to decrease the impedance and increase the corrosion.

2) The sulfur direct contact with metal surface is the direct reason that induces rapid corrosion and is also the indirect evidence that sulfur directly involved in corrosion electro-chemical reactions accelerates the corrosion process. The local corrosion caused by sulfur is closely related to the sulfur contact forms with materials.

3) At room temperature, the corrosion films consist of nickel sulfide (Ni_3S_2) and substrate alloy. However, when the temperature grows up to 90 °C, a lot of different types of

corrosion product appear, mainly including nickel sulfide (NiS), cubic pyrite (FeS_2), chromium oxide (Cr_2O_3) and nickel oxide (NiO). Sulfur is a strong oxidant, and the presence of sulfur leads to a serious localized corrosion.

References

1 Yu Man, Li Jingshe, Tang Haiyan *et al*. *Journal of Iron & Steel Research International*[J], 2011, 18(4): 68

2 Kritzer P, Boukis N, Dinjus E. *Corrosion-Houston*[J], 2000, 56(3): 265

3 Zhao X H, Han Y, Bai Z Q *et al*. *Electrochemical Acta*[J], 2011, 56(22): 7725

4 Petroleum and Natural Gas Industries-Materials for Use in H_2S-containing Environments in Oil and Gas Production-Part 3: Cracking-resistant CRAs (Corrosion-resistant Alloys) and Other Alloys, Switzerland standardization, ISO15156-3:2015[S]. Geneva (Switzerland): International Organization for Standardization, 2015

5 Montemor M F, Ferreira M G S, Hakiki N E *et al*. *Corrosion Science*[J], 2000, 42(9): 1635

6 Naffakh H, Shamanian M, Ashrafizadeh F. *Journal of Materials Processing Technology*[J], 2009, 209(7): 3628

7 Canut J M L, Maximovitch S, Dalard F. *Journal of Nuclear Materials*[J], 2004, 334(1): 13

8 Kanzaki M, Kitamura K, Hirohata N. *US Patent,* CA 2648711 C[P]. 2012

9 Ren C, Liu D, Bai Z *et al*. *Materials Chemistry & Physics*[J], 2005, 93(2-3): 305

10 Li D G, Feng Y R, Bai Z Q *et al*. *Applied Surface Science*[J], 2007, 253(20): 8371

11 Qian J S, Chen C F, Shen-Yi L I *et al*. *The Chinese Journal of Nonferrous Metals*[J], 2012, 22(8): 2214 (in Chinese)

12 Mcintyre N S. *Journal of the Electrochemical Society*[J], 1979, 126(5): 750

13 Huang J, Wu X, Han E H. *Corrosion Science*[J], 2010, 52(10): 3444

14 Angeliu T M, Was G S. *Cheminform*[J], 1993, 24(45): 1877

15 Carrette F, Lafont M C, Chatainier G *et al*. *Surface & Interface Analysis*[J], 2002, 34(1): 135

16 Chen C F, Fan C W, Zheng S Q *et al*. *The Chinese Journal of Nonferrous Metals*[J], 2008, 18(11): 2050 (in Chinese)

17 Zhao X H, Bai Z Q, Lin K *et al*. *Advanced Materials Research*[J], 2010, 152 (3): 1624

18 Zhou Q J, Zhang Z H, Yang J Q. *Baosteel Technical Research*[J], 2015, 9(4): 52

19 Tomio A, Sagara M, Doi T *et al*. *Corrosion Science*[J], 2014, 81(4): 144

20 Singh A, Lin Y, Liu W *et al*. *Journal of the Taiwan Institute of Chemical Engineers*[J], 2014, 45(4): 1918

21 Singh A, Lin Y, Liu W *et al*. *Journal of Industrial & Engineering Chemistry*[J], 2014, 20(6): 4276

22 Abboud Y, Abourriche A, Ainane T *et al*. *Chemical Engineering Communications*[J], 2009, 196(7): 788

23 Lebrini M, Robert F, Lecante A *et al*. *Corrosion Science*[J], 2011, 53(2): 687

24 Khamis A, Saleh M M, Awad M I. *Corrosion Science*[J], 2013, 66(1): 343

25 Chongdar S, Gunasekaran G, Kumar P. *Electrochemical Acta*[J], 2005, 50(24): 4655

26 Okuyama M, Haruyama S. *Chemischer Informationsdienst*[J], 1974, 5(12): 1

27 Sikora E, Macdonald D D. *Electrochemical Acta*[J], 2002, 48(1): 69

28 Macdonald D D, UrquidiMacdonald M. *Journal of the Electrochemical Society*[J], 1990, 137(8): 239

元素硫对 G3 合金在 H_2S+CO_2 饱和氯化物溶液中腐蚀行为的影响

范　舟[1]，王子瑜[1]，刘建仪[2]，黄泰愚[1]，赵　星[1]，胡晓刚[3]

(1. 西南石油大学，四川 成都 610500)

(2. 油气藏地质及开发工程国家重点实验室，四川 成都 610500)

(3. 重庆惠科金渝光电科技有限公司，重庆 401346)

摘　要：利用电化学显微镜（SECM）、扫描电子显微镜（SEM）和电化学阻抗谱（EIS）研究了镍基合金 G3 在室温（25 ℃）和高温（90 ℃）含 H_2S、CO_2，Cl^-的介质环境中各种硫状态下的腐蚀行为。结果表明，随温度升高，腐蚀变得更加严重，镍基合金 G3 表面出现轻微的点蚀；阳极极化曲线在室温下具有钝化区，而在 90 ℃的温度下出现活性溶解区，钝化现象消失。物相分析表明，在镍基合金 G3 上形成的钝化膜主要由 Ni、Cr 及 Fe 的氧化物组成，由于 S^{2-}侵入薄膜，导致钝化膜溶解，腐蚀产物由 NiS、FeS_2 组成。G3 合金在含硫环境中的耐腐蚀性减弱，与沉积硫、析出硫相比较，悬浮硫状态下，镍基合金 G3 表面钝化膜最致密，腐蚀最轻微。研究表明，硫是强氧化剂，其存在导致严重的局部腐蚀，元素硫的状态是影响腐蚀产物膜的致密性和生长速率的关键因素，也是影响合金腐蚀速率的关键因素。

关键词：镍基合金 G3；腐蚀行为；极化曲线；阻抗谱；钝化膜；腐蚀形貌

作者简介：范　舟，男，1971 年生，硕士，副教授，西南石油大学材料科学与工程学院，四川 成都 610500，电话：028-83037406，E-mail: fanzhou505@163.com